Several Factors Affecting Faster Rates of Gibbsite Formation

Y. Cesteros,† P. Salagre,† F. Medina,‡ and J. E. Sueiras*,‡

Facultat de Química and Escola Tècnica Superior d'Enginyeria, Universitat Rovira i Virgili, Pl. Imperial Tarraco, 1, 43005 Tarragona, Spain

Received July 23, 1998. Revised Manuscript Received November 3, 1998

A rigorous study of the experimental conditions for the obtention of several aluminum hydroxide gels was performed. To obtain different alumina hydrate phases, some of the key factors which affect the rates of formation like precipitation temperature, ammonia concentration, and aging and pH conditions were studied. The alumina hydrates obtained such as amorphous gels, boehmite, bayerite, and gibbsite were calcined under controlled conditions, to yield the final δ- and α-aluminas. Either the intermediate alumina hydrates or the final alumina oxides were structurally characterized using SEM, TG, XRD, and nitrogen physisorption (BET areas and pore distributions) techniques in order to understand the key factors that control faster rates of hydrates formation. Large amounts of gibbsite were obtained under aging times of 1 week, compared with the reported several months. Then, pure α-Al_2O_3 with surface areas of about 40 m^2/g was easily obtained from gibbsite. α-Al_2O_3 with less than 10 m^2/g was usually obtained from bayerite.

Introduction

Alumina and its hydrates (hydroxides and oxihydroxides) are commercially important materials due to their use as ceramics and catalyst supports.

γ-AlO(OH) (boehmite) may be a precursor of α-AlO(OH) (diaspore) on a geological scale, but diaspore can only be obtained in the laboratory at high temperatures and pressures. Typical features of the α-Al_2O_3 obtained from diaspore by calcination are high stability and high surface area (70 m^2/g).[1]

Differences in surface energy can favor the formation of a particular alumina polymorph in the nanocrystalline region. Then, nanosized corundum of higher surface area (160 m^2/g) from precursor diaspore and energetically more stable γ phase relative to corundum at surface areas greater than 125 m^2/g were reported by Perrotta et al.[2,3] In regard with the diaspore route to corundum, Perrotta and co-workers claim a two-step transformation sequence from the formation of a monoclinic α'-Al_2O_3 intermediate, which is responsible of a fast and high conversion process to corundum in the presence of moist air at elevated temperatures.[4,5]

The dehydration of the alumina hydrates during calcination has been examined using a wide variety of techniques, and the alumina hydrates (boehmite, bayerite, and gibbsite) are eventually transformed into the extremely stable α-alumina or corundum.[6−21] The number of dehydration paths depend on a number of factors, including particle size, moisture, alkalinity, pressure, bed depth, heating rate, and preparation method.[20,21] Likewise, the aging of the gels is a parameter that can give alumina hydrates with different textural and surface properties. Some studies have been done on the gel hydroxide evolution (aging) under different pH conditions.[21,22] Mathieu[23] has proposed Scheme 1, where a fast transformation into boehmite is reached on maintaining the gel in its precipitating solution (basic medium). However, the evolution of this boehmite, first to bayerite and eventually to gibbsite, takes a longer time. Gyani[24] also observed that the gels obtained from aluminum salts under basic conditions crystallize quickly

* To whom correspondence should be addressed.
† Facultat de Química.
‡ Escola Tècnica Superior d'Enginyeria.

(1) Tsuchida, T.; Ohta, S.; Horigome, K. *J. Mater. Chem.* **1994**, *4* (9), 1503.
(2) McHale, J. M.; Auroux, A.; Perrotta, A. J.; Navrotsky, A. *Science* **1997**, *277*, 788.
(3) Perrotta, A. J. *Mater. Res. Innovat.* **1998**, *2*, 33.
(4) Carim, A. H.; Rohrer, G. S.; Dando, N. R.; Tzeng, S. Y.; Rohrer, C. L.; Perrotta, A. J. *J. Am. Ceram. Soc.* **1997**, *80* (10), 2677.
(5) Perrotta, A. J.; Minnick, J. B. U.S. Patent 5,334,366, 1994.
(6) Tertian, R.; Papee, D. *J. Chem. Phys.* **1958**, *55*, 341.
(7) Saalfeld, H. N. *Jb. Miner. Abh.* **1960**, *95*, 1.
(8) Lippens, B. C.; de Boer, J. H. *Acta Crystallogr.* **1964**, *17*, 1312.
(9) Beretka, J.; Ridge, M. J. *J. Chem. Soc (A)* **1967**, 2106.
(10) Wilson, S. J. *Proc. Br. Ceram. Soc.* **1979**, *28*, 281.
(11) Rouquerol, J.; Rouquerol, F.; Ganteaume, M. *J. Catal.* **1979**, 57.
(12) Sato, T. *J. Chem. Technol. Biotechnol.* **1981**, *31*, 670.
(13) Sato, T.; Suzuki, M.; Ikoma, S. *J. Chem. Technol.Biotechnol.* **1981**, *31*, 745.
(14) Naumann, R.; Koehnke, K.; Paulik, J.; Paulik, F. *Thermochim. Acta* **1983**, *64* (1−2), 1.
(15) Dexpert, H.; Larne, J. F.; Mutin, I.; Moraweck, B.; Bertaud, Y.; Renouprez, A. *J. Metal.* **1985**, *37*, 17.
(16) Chunkin, G. D.; Seleznev, Y. L. *Inorg. Mater.* **1987**, *23*, 374.
(17) Jayaram, V.; Levi, C. G. *Acta Metall.* **1989**, *37*, 569.
(18) Sato, T. *J. Therm. Anal.* **1987**, *32*, 61.
(19) Slade, R. C. T.; Southern, J. C.; Thompson, I. M. *J. Mater. Chem.* **1991**, *1* (4), 563.
(20) Slade, R. C. T.; Southern, J. C.; Thompson, I. M. *J. Mater. Chem.* **1991**, *1* (5), 875.
(21) Pascal, P.; Chretien, A.; Trambouze, Y.; Hutter, J. C.; Freundlich, W. In *Nouveau Traité de Chimie Minérale*; Masson et Cie: Paris, 1963; Vol 6, p 574.
(22) Zhdanov, G. S.; Razmanova, Z. P. *Comm. Acad. Sci. URSS* **1951**, *15*, 202.
(23) Mathieu, M. V., Ph.D. Thesis., Fac. Sci. Univ. Lyon, 1956.
(24) Gyani, B. P. *J. Phys. Chem.* **1952**, *56*, 762.

10.1021/cm980527z CCC: $18.00
Published on Web 12/24/1998

Scheme 1

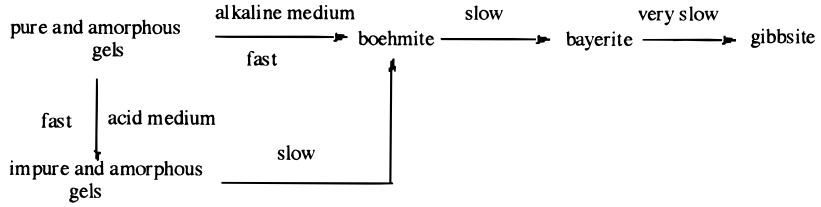

Scheme 2

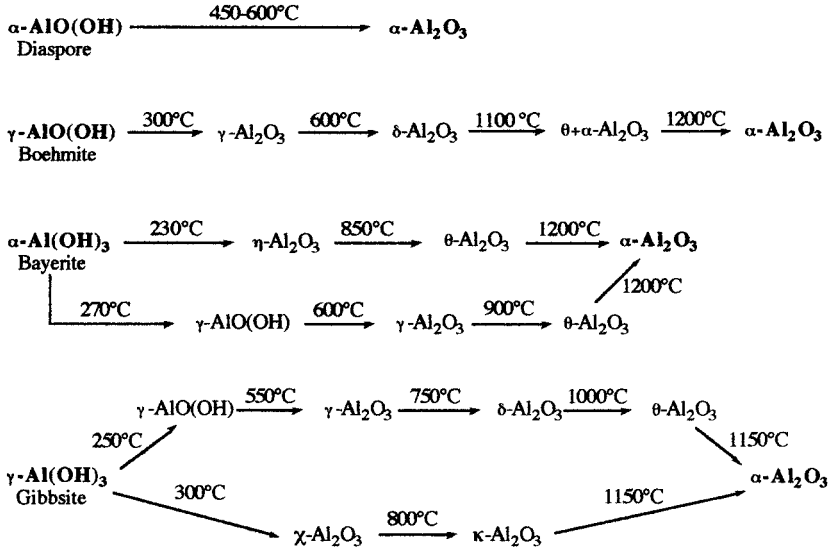

in the precipitation medium, whereas they evolve slowly if acetic acid is added.

Scheme 2 shows the generally accepted thermal sequences for the transformation of aluminum hydrates in air.[19,21,25,26] On the whole, the total transformation needs temperatures higher than 1100 °C and the result is an α-Al_2O_3 of low surface area (about 1−5 m^2/g).[27,28] On the other hand, the gibbsite phase seems to have a lower transition temperature.[29]

The aim of this work is the study of the phases involved and the key factors affecting the formation rates of gel hydroxides and their transformations to corundum, by controlling gel preparation conditions such as precipitation temperature, ammonia concentration, gel aging, and pH. The textural and structural properties of the different α-Al_2O_3 precursors obtained should be related to these preparation conditions.

Experimental Section

Gel Preparation. One series of gel hydroxides (G_1−G_6) was prepared from the precipitation of a 0.1 M aluminum nitrate hexahydrate aqueous solution with ammonia aqueous solutions of several concentrations at 25 and 75 °C (Table 1). The gels obtained were washed and dried overnight in an oven at 120 °C.

Table 1. Preparation Conditions of the Alumina Gels

gel	[NH_3] (%)	precipitation temp (°C)
G_1	12.5	25
G_2	12.5	75
G_3	5.0	25
G_4	5.0	75
G_5	0.5	25
G_6	0.5	75

Table 2. Aging Conditions of the Gels G_2, G_4, and G_6 and XRD Characterization of the Aged Gels Obtained

	first step[a]		second step[b]			
gel detected	pH	time (days)	pH	time (days)	aged gel	cryst phases (XRD)
G_2	8	14			I_2	boehmite
G_4	8	14			I_4	bayerite
G_6	8	14			I_6	bayerite
G_2	8	7	7	7	J_2	boehmite
G_4	8	7	7	7	J_4	bayerite
G_6	8	7	7	7	J_6	bayerite
G_2	8	7	7	35	K_2	bayerite
G_6	8	7	7	35	K_6	bayerite
G_6	8	7	2	1/3	L_6	gibbsite
G_6	8	7	2	1	M_6	gibbsite

[a] Gel maintained in its precipitating solution. [b] pH adjusting with 6% HNO_3 solution.

Gels G_2, G_4, and G_6 obtained at the higher precipitation temperature (75 °C) and at a calcination temperature of 950 °C for 1.30 h, showed a greater tendency to evolve to the α-alumina phase. For this reason those G2, G4, and G6 gels were chosen as the starting material to study the effect of the aging process on the formation of α-Al_2O_3 (see Table 2).

The gels labeled I_2, I_4, and I_6 were aged in their precipitating solutions (pH = 8) for 14 days (first step in Table 2), whereas the gels labeled J_2, J_4, J_6, K_2, K_6, L_6, and M_6 were obtained in two steps by modifying the pH and aging time (first + second steps in Table 2).

(25) Lippens, B. C.; Steggerda, J. J. *Physical and Chemical Aspects of Adsorbents and Catalysts*; Linsen, B. G., Ed.; Academic Press: New York, 1970.
(26) Morterra C.; Magnacca, G. *Catal. Today* **1996**, *27*, 497.
(27) Medina, F.; Salagre, P.; Fierro, J. L. G.; Sueiras, J. E. *J. Chem. Soc. Faraday Trans.* **1993**, *89* (21), 3981.
(28) Oberlander, R. K. *Applied Industrial Catalysis*; Leach, B. E., Ed.; Academic Press: New York, 1984.
(29) Greenwood, N. N.; Earnshaw, A. *Chemistry of the Elements*; Pergamon Press: Oxford, 1984; Vol 3.

The results of these studies show that importnt variables that affect the evolution of the gels are pH and aging time. The gels obtained were washed to pH = 7 and dried overnight in an oven at 120 °C.

Alumina Preparation. Several aluminas were obtained from the calcination of the gels previously prepared. The calcination procedures were performed in a furnace at 950 °C under air for 1.30, 4.30, and 6 h.

The nomenclature used to refer to the aluminas will be the name of the initial gel and the calcination time (hours in parentheses) at 950 °C; i.e., G_1(1.30) corresponds to the alumina obtained by calcining the G_1 gel at 950 °C for 1.30 h.

Scanning Electron Microscopy (SEM). The scanning electron micrographs were obtained with a JEOL JSM-35C scanning microscope operating at an accelerating voltage of 30 kV, a work distance (wd) of 39 mm, and magnification values in the range of 100−200×.

Thermogravimetric Analysis (TG). Thermal decompositions of alumina hydrates were carried out in a Perkin-Elmer TG 7 microbalance, with an accuracy of 1 μg, equipped with a 0−1000 °C programmable temperature furnace. Each sample (50 mg) was heated in a N_2 flow (80 cm^3/min) from 50 to 900 °C at 10 °C min^{-1} and maintained at 900 °C for 1.30 h. The weight change obtained is a measure of the water loss of the sample after calcination.

X-ray Diffraction (XRD). Powder X-ray diffraction (XRD) patterns were obtained with a Siemens D-5000 diffractometer using a nickel-filtered Cu Kα radiation. The patterns were recorded over a range of 2θ angles from 5° to 85° and they were compared with the X-ray powder files to confirm the phase identities. This technique was also used to determine the percentage of α-Al_2O_3 in completely crystalline mixtures of δ-Al_2O_3 + α-Al_2O_3 by the Rietveld method.[30] This method enables a quantitative phase analysis of multicomponent mixtures to be made from the X-ray powder diffraction data, provided no amorphous materials are present.

BET Areas and Pore Distributions. The BET surface areas of the different samples were calculated from the nitrogen adsorption isotherms at 77 K using a Micromeritics ASAP 2000 surface analyzer and assuming a nitrogen molecule cross section of 0.164 nm^2. The same equipment automatically calculates the pore distribution of the solids for pore diameters between 10 and 3000 Å using the Barrett, Joyner, and Halenda (BJH) method.[31]

Results and Discussion

Our observations show that certain preparation parameters, like precipitation temperature of the gels, ammonia concentration, gel aging, and pH, strongly affect the bulk and surface structures of the aluminas obtained. Small changes of these parameters lead to different alumina hydrate phases that evolve to different aluminas after calcination. The results obtained are discussed below.

Scanning Electron Microscopy (SEM). In an attempt to correlate the particle sizes with the evolution of the gels toward the α-Al_2O_3 phase, the SEM technique was used. Therefore, we estimated here the particle sizes taken from the SEM pictures and the magnification parameters.

Figures 1, 2 and 3 show the scanning electron micrographs of the gels G_1, G_2, and G_6, respectively. If we compare G_1 and G_2, which were prepared with the same concentration of ammonia (12.5%), we find that the particle sizes of the gel precipitated at 75 °C (G_2) are smaller than those from the precipitate at 25 °C (G_1).

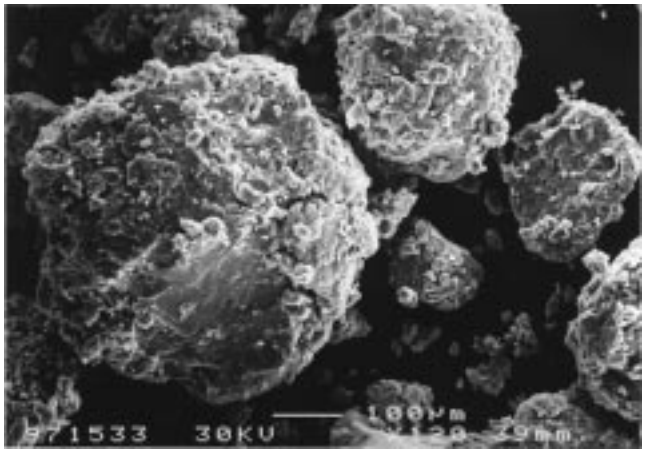

Figure 1. Scanning electron micrograph of the gel G_1.

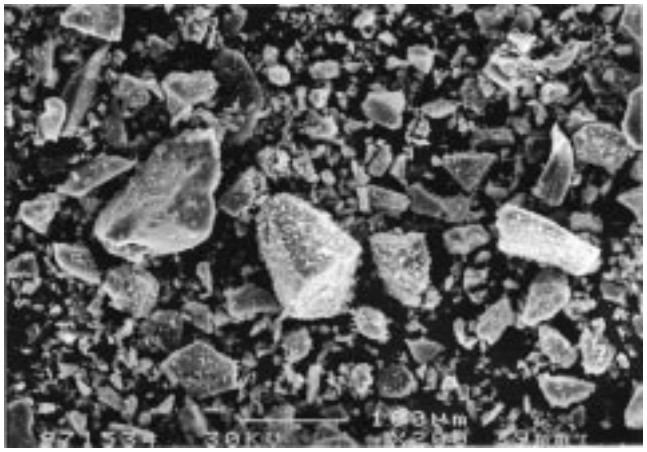

Figure 2. Scanning electron micrograph of the gel G_2.

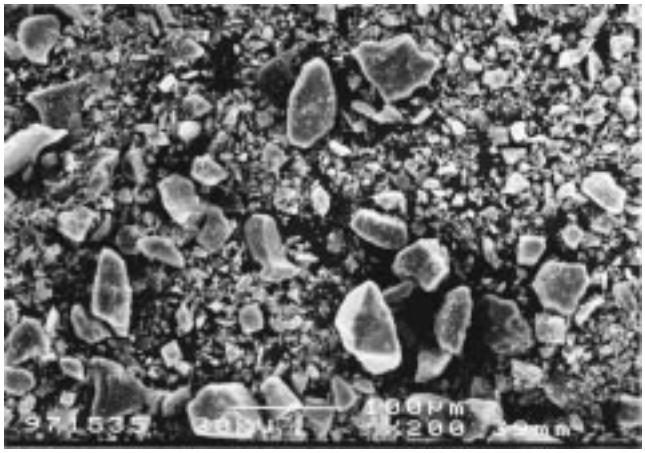

Figure 3. Scanning electron micrograph of the gel G_6.

On the other hand, if we compare the gels G_2 and G_6, both precipitated at 75 °C but with different ammonia concentrations (Table 1), we can see that the particle sizes of the gel G_6 are smaller than those from gel G_2. The gels with smaller particle sizes are found to evolve more efficiently to the α-Al_2O_3 phase after calcination, as is shown below (see Table 3), probably because nucleation and diffusion rates are favored by the large grain boundary areas available in fine-grained powders with small particle sizes.

Thermogravimetric Analysis (TG). Another parameter, studied by TG, was the loss of water from the gels. Figure 4 shows the TG plot for the samples G_1 and

(30) Rietveld, H. A. *J. Appl. Cryst.* **1969**, *2*, 65.
(31) Barrett, E. P.; Joyner, L. G.; Halenda, P. P. *J. Am. Chem. Soc.* **1951**, *73*, 373.

Table 3. BET Areas of the Aluminas Obtained after Calcination at 950 °C for 1.30 Hours

alumina	BET area (m^2/g)	phases (XRD)
$G_1(1.30)$	93	δ-Al_2O_3
$G_3(1.30)$	101	δ-Al_2O_3
$G_5(1.30)$	114	δ-Al_2O_3
$G_2(1.30)$	98	δ- + α-Al_2O_3 (2%)[a]
$G_4(1.30)$	77	δ- + α-Al_2O_3 (10%)[a]
$G_6(1.30)$	56	δ- + α-Al_2O_3 (25%)[a]

[a] α-Al_2O_3 content, in parentheses, determined by the Rietveld method.[26]

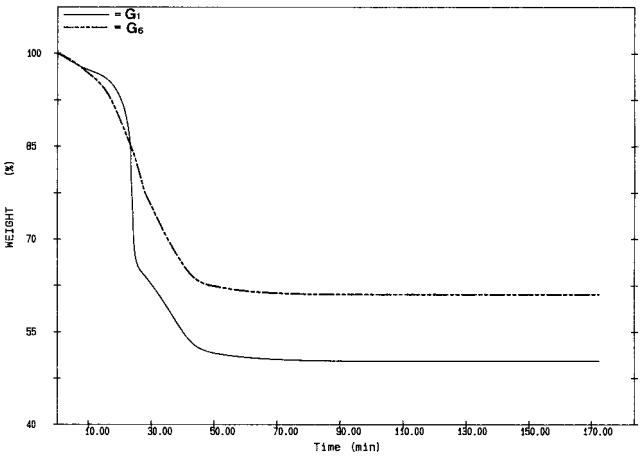

Figure 4. TG plot of change in weight percent vs time for the gels G_1 and G_6.

G_6 under the conditions given in the Experimental Section. The gel G_6, which after calcination shows a higher content of the α-Al_2O_3 phase, undergoes a smaller loss of total water.

Therefore, the ammonia concentration and the precipitation temperature exert two important and opposite effects on the gel obtained and consequently on the kind of alumina formed after the calcination of the gels. When the ammonia concentration used in the precipitation procedure is high, the gel loses more water and larger particles are obtained, whereas if the precipitation temperature is high, the gel loses less water and yields smaller particles.

When the gels have low water content and consequently are made of small particles, the structure of the gel evolves more quickly toward the α-Al_2O_3 phase, as confirmed below from the XRD results.

X-ray Diffraction (XRD) and Aging. The XRD patterns of the gels G_1−G_6, before calcining, showed amorphous phases, as expected from the precipitation method used. No differences were observed among the XRD patterns, although the gel particle sizes appeared somewhat smaller when the ammonia concentration used was low.

After calcining the gels at 950 °C for 1.30 h, we obtained several aluminas whose diffraction lines are plotted in Figures 5 and 6.

The aluminas $G_1(1.30)$, $G_3(1.30)$, and $G_5(1.30)$, obtained from the calcination of the gel precipitated at 25 °C (Table 3 and Figure 5), were identified as poorly crystallized δ-Al_2O_3. On the other hand, the aluminas $G_2(1.30)$, $G_4(1.30)$, and $G_6(1.30)$, obtained from the calcination of the gel previously precipitated at 75 °C, gave the diffraction lines of α-Al_2O_3 and δ-Al_2O_3 phases (see Table 3 and Figure 6). The 2θ angles of these

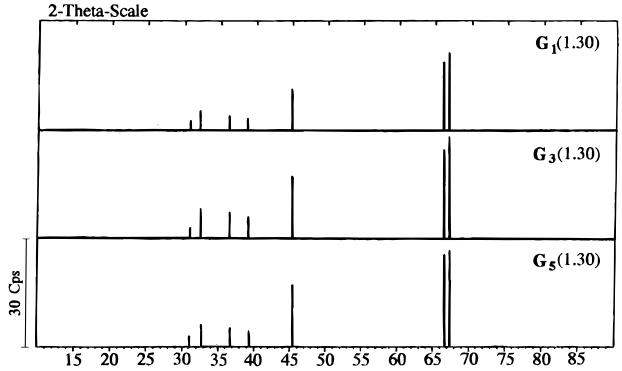

Figure 5. X-ray diffraction lines of the aluminas obtained from the calcination (950 °C) of the gels precipitated at 25 °C.

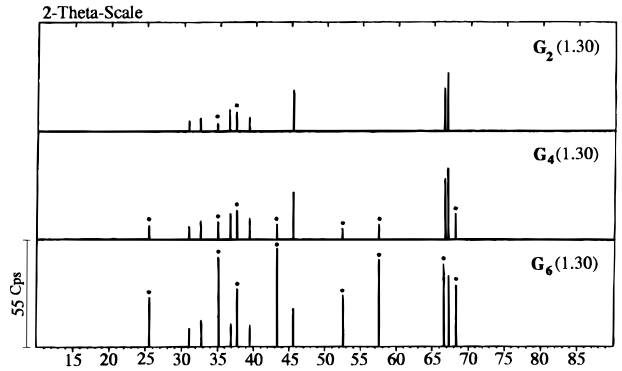

Figure 6. X-ray diffraction lines of the aluminas obtained from the calcination (950 °C) of the gels precipitated at 75 °C: ●, α-Al_2O_3.

crystalline phases, with the relative intensities in parentheses, are summarized as follows: 31.14 (40), 32.78 (80), 36.96 (60), 39.49 (40), 45.55 (80), 66.76 (60), and 67.31 (100) for the δ-Al_2O_3 phase; 25.58 (75), 35.14 (90), 37.78 (40), 43.36 (100), 52.55 (45), 57.52 (80), 66.55 (30), and 68.20(50) for the α-Al_2O_3 phase.

Aging is the spontaneous evolution of a gel structure which results from an ordering of its crystalline state. This evolution varies according to the initial gel, the pH, and time of aging.[16,17] These parameters have been studied for the gels G_2, G_4, and G_6 under the conditions shown in Table 2. This table also shows the XRD phases obtained after the aging treatment. The 2θ angles (with the relative intensities in parentheses) for the different phases identified are also summarized as follows: 14.48 (100), 28.18 (65), 38.34 (55), and 48.93 (30) for the boehmite phase; 18.83 (90), 20.40 (70), 27.86 (30), 40.57 (100), and 53.11 (40) for the bayerite phase; 18.28 (100) and 20.30 (16) for the gibbsite phase.

The gel I_2 was obtained after aging the gel G_2 for 2 weeks in its precipitating solution at pH = 8, then a new crystalline phase, boehmite (γ-AlO(OH), was detected by XRD. When the aging is carried out for 1 week at pH = 8 and a second week at pH = 7 (gel J_2) the amount of boehmite increases, and if the second step is increased to 5 weeks at pH = 7 (gel K_2), the bayerite phase (α-$Al(OH)_3$) can be identified.

Gels G_4 and G_6 were somewhat different than G_2. After the aging treatment at pH = 8 for 2 weeks (gels I_4 and I_6), the bayerite peaks were detected. The bayerite content increases when both gels are aged for 1 week under pH = 8 followed by 1 more week at pH = 7 (gels J_4 and J_6). It should be pointed out that the

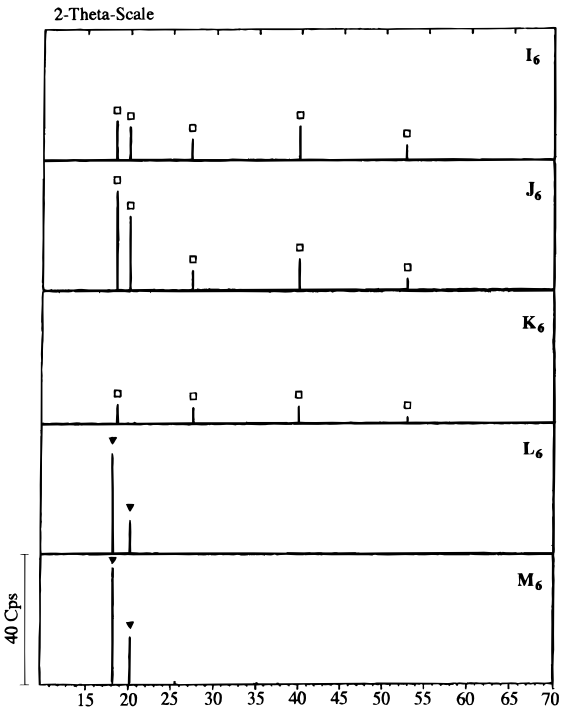

Figure 7. X-ray diffraction lines of the aluminum hydrates obtained by aging gel G_6: □, bayerite; ▼, gibbsite.

amount of bayerite phase obtained by the different aging procedures tested is always bigger when starting from the gel G_6, showing that this gel exhibits a faster evolution to the bayerite phase. Several new aging procedures, which involve increasing the aging time and the acidic conditions, were performed to study the evolution of G_6 (see Table 2).

Figure 7 shows the XRD results for gel G_6 under different aging conditions. When the aging time at pH = 7 is increased to 5 weeks (gel K_6) a new evolution of the gel was observed. The XRD shows that the peaks of bayerite partially disappear. This may be interpreted in terms of the gel transformation to a new gibbsite (γ-$Al(OH)_3$) phase. As we have seen previously, the pH has a considerable influence on the evolution of the gels. Then, pH conditions for the second step were modified to pH = 2. When gel G_6 is aged for 1 week in its precipitating solution at pH = 8 and then at pH = 2, the gibbsite phase shows up after 8 h (gel L_6), and if this aging time at pH 2 is raised to 1 day (gel M_6), the gibbsite peak intensities increase parallelly (Figure 5). Those observations are in agreement with Scheme 1.

BET Areas and Pore Distributions. The BET surface areas and the crystalline phases described above for these aluminas are given in Table 3. The aluminas obtained from the gels precipitated at 25 °C have higher BET area values when the ammonia concentration used is lower. The later may be due to the formation of small particles when the precipitation is carried out under these conditions, which is in agreement with the XRD results. In contrast, the aluminas obtained by calcination had lower BET area values when the precipitation temperature was 75 °C and the ammonia concentration decreased, which may be interpreted in terms of the presence of α-Al_2O_3 (see Table 3 and Figure 6). The specific surface area decreases when the content of α-Al_2O_3 in the sample increases, according to the characteristic lower surface area of this phase.

Table 4. Surface Characterization of Several Aluminas by Nitrogen Physisorption and XRD

alumina	phases detected (XRD)	BET area (m^2/g)	pore volume[a] (cm^3/g)	average pore diameter[a] (Å)
$G_1(0.30)$	δ-Al_2O_3	96	0.25	70
$G_1(1.30)$	δ-Al_2O_3	93	0.23	52
$G_6(0.30)$	δ-Al_2O_3	74	0.14	44
$G_6(1.30)$	δ- + α-Al_2O_3	69	0.12	31
$G_6(6.00)$	α-Al_2O_3	23	0.12	120

[a] Calculated by the machine software from the method of Barret, Joyner, and Halenda.[27]

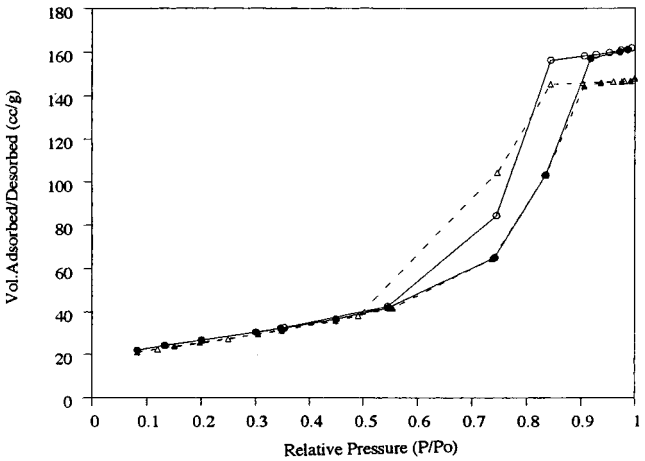

Figure 8. Plot of the nitrogen adsorption (full symbols)/desorption (empty symbols) isotherms at 77 K for the aluminas $AG_1(0.5)$ (○, ○) and $AG_1(1.5)$ (△, △).

From these results it appears interesting to find out why different final phases are obtained after calcination, depending on the precipitation temperature of the gels. These differences may depend on the different rates of evolution to α-Al_2O_3 or on the different sequences (different transition species) in the process of obtention of the α-Al_2O_3 phase.

To try to answer this question, a study was carried out on the adsorption−desorption isotherms and the pore distributions of the aluminas obtained by calcining the gels G_1 and G_6 at 950 °C for 0.5 h [$G_1(0.30)$, $G_6(0.30)$] and 1.5 h [$G_1(1.30)$, $G_6(1.30)$] using the nitrogen adsorption technique. Previously, $G_1(0.30)$ and $G_6(0.30)$ were identified by XRD as δ-Al_2O_3, the same as $G_1(1.30)$, whereas the sample $G_6(1.30)$ was a δ-/α-Al_2O_3 mixture. These diffraction results are shown in Table 4.

Furthermore, Figure 8 shows the nitrogen adsorption−desorption isotherms for the aluminas obtained from gel G_1, and Figure 9 shows the nitrogen adsorption−desorption isotherms for the aluminas obtained from gel G_6. Figure 10 shows the pore distributions, according to the BJH method,[31] as the plot of $dV/d(\log D)$ desorption pore volume (V) vs pore diameter (D) for the samples of calcined products obtained from G_1 and G_6 (including the alumina $G_6(6.00)$ that is pure α-Al_2O_3). Some data such as the BET area, pore volume, and average pore diameter can also be obtained from those plots (Table 4).

The isotherms in Figure 8 can be identified as type IV according to the classification of Brunauer, Deming, Deming, and Teller (BDDT),[32] characteristic of a mesoporous material. The shift of the hysteresis loop at lower

Scheme 3

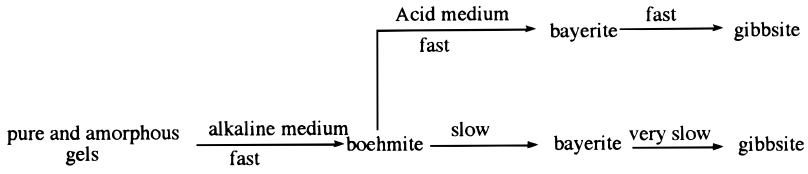

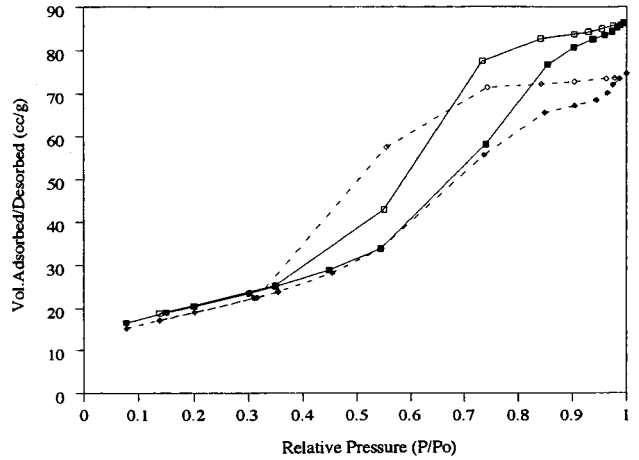

Figure 9. Plot of the nitrogen adsorption (full symbols)/ desorption (empty symbols) isotherms at 77 K for the aluminas $AG_6(0.5)$ (■, □) and $AG_6(1.5)$ (◆, ◇).

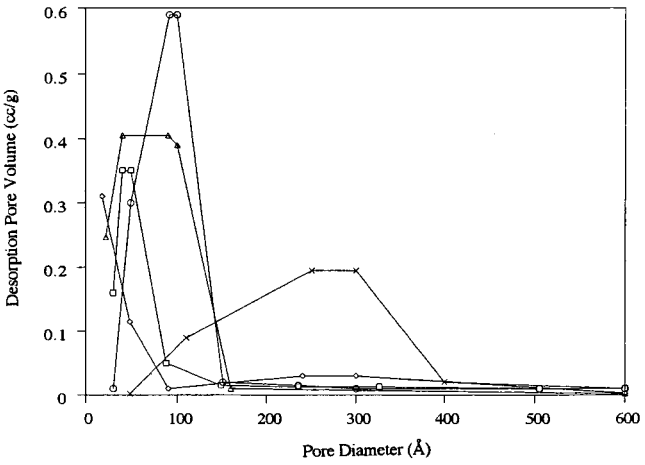

Figure 10. Pore distribution plot for the aluminas $AG_1(0.5)$ (○), $AG_1(1.5)$ (△), $AG_6(0.5)$ (□), $AG_6(1.5)$ (◇), and α-Al_2O_3 (×).

relative pressures in the alumina $G_1(1.30)$ is in agreement with the relative increase in the content of smaller pores, as can be seen in Figure 10. The pore distribution plots of samples $G_1(0.30)$ and $G_1(1.30)$ show the absence of porosity between 200 and 600 Å, which is the characteristic region of materials such as the α-Al_2O_3 phase.

The isotherms from samples $G_6(0.30)$ and $G_6(1.30)$ (Figure 9) can also be classified as type IV isotherms with a desorption plot shifted toward lower relative pressures for the alumina $G_6(1.30)$. That may be accounted for by the fact that the pores are smaller than in samples $G_1(0.30)$ and $G_1(1.30)$ (Figure 10), and it should be related to the presence of α-Al_2O_3 phase in the sample $G_6(1.30)$, as well.

Similarly, the data in Table 4 confirm that the samples $G_1(0.30)$, $G_1(1.30)$, $G_6(0.30)$, and $G_6(1.30)$ undergo different steps in the transformation process from δ-Al_2O_3 to α-Al_2O_3. Compared to the aluminas prepared from G_6, those prepared from G_1 show higher surface area, mesoporosity, and total pore volume. The porosity was evaluated from the average pore diameter obtained from the desorption data by the BJH method.[31] The pore distribution shows that sample $G_6(1.30)$ contains small amounts of a new mesoporous material with a larger pore diameter, probably related to the presence of the α-Al_2O_3 phase (Figure 10). The $G_6(6.00)$ pore diameter was clearly found to increase in the 200−400 Å range of the pore size distribution plot. It seems that $G_6(1.30)$ evolves to the α-Al_2O_3 phase.

Table 5. BET Areas of the α-Al_2O_3 Obtained from the Calcination of the Gels at 950 °C

α-Al_2O_3	calcination time (h)	BET area (m^2/g)
$G_6(6.00)$	6.00	23
$K_6(6.00)$	6.00	26
$L_6(4.30)$	4.30	38
$M_6(3.00)$	3.00	42

These results suggest that the four samples are intermediate compounds in the step-by-step transformation of δ-Al_2O_3 into the α-Al_2O_3 phase according to the following scheme:

$$G_1(0.30) \rightarrow G_1(1.30) \rightarrow G_6(0.30) \rightarrow G_6(1.30) \rightarrow \alpha\text{-}Al_2O_3$$

Only the presence of δ-Al_2O_3 and α-Al_2O_3 phases have been detected from the evolution of these gels, as can be shown by the XRD spectra.

Table 5 shows the BET areas of the α-Al_2O_3 obtained from different aged G6 gels. Larger surface areas (where sintering is minimized) are obtained at shorter calcination times. Only those experimental procedures which enable the obtention of α-Al_2O_3 in a short time are suitable for the obtention of α-Al_2O_3 with larger surface areas.

NH_3 Concentration, pH, and Aging. To obtain the boehmite in a shorter time, the alkaline medium path is recommended first. Then, at this point, bayerite and gibbsite are obtained faster and in greater amounts the more acidic the pH of the solution is (Scheme 3), allowing the gel M_6 (aged from G_6 for 1 week in its precipitating solution and then for 1 more day under acidic pH) to yield the most gibbsite.

Thus, bayerite and gibbsite are obtained in a significantly shorter time than is found in the literature, where aging times of several weeks to obtain bayerite and some months to obtain gibbsite have been reported.[21]

Another point which is worth emphasizing is that aging is faster in gel G_6, obtained from precipitation with the lower concentration of ammonia (0.5%), and it is slower, under the same conditions, for the gels obtained by precipitation with a larger concentration

(32) Brunauer, S.; Deming, L. S.; Deming, W. S.; Teller, E. *J. Am. Chem. Soc.* **1940**, *62*, 1723.

of ammonia. This effect can also be explained in terms of the smaller particle size observed in gel G_6 (see Figure 3), as nucleation and diffusion rates are faster for smaller particles.

All the aged gels prepared from G_2, G_4, and G_6 were calcined at 950 °C for 1.30 h. Consequently, the obtained aluminas, $I_2(1.30)$, $I_4(1.30)$, $I_6(1.30)$, $J_2(1.30)$, $J_4(1.30)$, $J_6(1.30)$, $K_2(1.30)$, $K_6(1.30)$, $L_6(1.30)$, and $M_6(1.30)$ show α-Al_2O_3 contents in the following decreasing orders, depending on the starting gel: $J_2(1.30) \approx K_2(1.30) > I_2(1.30) > G_2(1.30)$; $G_4(1.30) > I_4(1.30) > J_4(1.30)$; and $M_6(1.30) > L_6(1.30) > K_6(1.30) > G_6(1.30) > I_6(1.30) > J_6(1.30)$.

From these results we can conclude that the ease of obtention of the α-Al_2O_3 phase from gel calcination obeys the following order: gibbsite > boehmite > amorphous gel > bayerite.

Conclusions

Experimental conditions, like precipitation temperature, ammonia concentration, aging, and pH, that affect the rates of formation of several aluminum hydrates were studied. The alumina hydrates obtained such as amorphous gels, boehmite, bayerite, and gibbsite were calcined under controlled conditions, eventually obtaining δ- and α-aluminas. Either the intermediate alumina hydrates or the calcined alumina oxides were structurally characterized. SEM pictures show the smaller particle sizes of those gels prepared under hot precipitation and lower ammonia concentration. The results from the TG analysis indicate smaller losses of water in gels with smaller particle sizes. The XRD technique detects the presence of crystalline phases of gibbsite, bohemite, and bayerite from the aluminum hydrates and δ-Al_2O_3 and α-Al_2O_3 from the calcined hydrates. Gibbsite is more easily obtained from gels with the smaller particle sizes, and α-Al_2O_3 is more easily obtained from gibbsite. The nitrogen physisorption experiments (BET and pore distributions) show larger surface areas at short calcination times, for these types of mesoporous materials. Pure α-Al_2O_3 with surface areas of about 40 m^2/g was easily obtained from gibbsite, whereas α-Al_2O_3 with surface areas of less than 10 m^2/g was usually obtained from bayerite.

The rate of gibbsite formation is found to be faster if (a) the gel precursor is prepared by hot precipitation, (b) the ammonia concentration is low, and (c) the gel is first aged in basic medium and then in acid medium, since this aging procedure enables the initial amorphous gel to evolve to gibbsite in a short time. It has been shown that the calcination of gibbsite allows transformation into α-Al_2O_3 faster and with higher surface area than the other alumina hydrates. The method described in this report enables α-Al_2O_3 to be prepared with a high surface area, an easier preparation procedure, and temperatures and calcination times which are milder and shorter than other conditions previously reported.[21,1]

CM980527Z